Cranz-Schardin Visualisation of a Hypersonic Cone with Gas Injection

David R. Buttsworth, David B. T. Sercombe
Faculty of Engineering and Surveying, University of Southern Queensland, AUSTRALIA, 4350

ABSTRACT

We have developed a five-picture Cranz-Schardin system for Schlieren flow visualization on a gun tunnel facility at the University of Southern Queensland to aid the study of unsteady shock systems in nominally steady hypersonic flows. The system produces useful images at framing rates up to about 1 MHz even though the system development was constrained by a very modest budget. The system uses multiple LED light sources driven by an in-house designed device that delivers a high current pulse to each LED with a programmable time delay between each pulse. The images are captured using four separate, black and white video devices and one digital still camera. The utility of the system is demonstrated by imaging gas injection from an annulus on a 10 degree half angle cone positioned at the exit of the contoured Mach 7 nozzle. Visualisation of the cone without gas injection demonstrates that the half angle of the conical shock is approximately 13.9 degrees (the Taylor-Maccoll conical shock angle at Mach 7 for an inviscid cone half angle of 10 degrees is 12.9 degrees). The gas injection condition used in these experiments disturbed the flow field upstream of the injection point to such an extent that the thickness of the shocked flow at the point of injection was larger than the no-injection case by a factor of approximately two. The conical shock angle in the case of injection increased to approximately 19 degrees, and a variation in this shock angle of approximately 1 degree was observed during the nominally steady, facility run time.

Keywords: Cranz-Schardin, hypersonic cone, gas injection, LED pulsed light source

1. INTRODUCTION

To facilitate the development of new aerospace transportation systems and cost-effective space exploration missions with an atmospheric entry component, hypersonic flow research is required. For the correct simulation of the high temperature physics usually associated with such flows, it is important to duplicate the flow energy of the full-scale configuration.

A number of wind tunnel facilities with the capacity to correctly duplicate the high enthalpy flows associated with hypersonic flight within terrestrial and extraterrestrial atmospheres already exist in Australia. For example, the T4 shock tunnel produces flows with stagnation enthalpies between about 3 and 13 MJ/kg and the X-series of expansion tubes produce enthalpies up to 100 MJ/kg. These high energy flows are produced for short periods of time and generally the period of useful test flow decreases with increasing enthalpy. A review of such facilities is presented by Stalker (2006).

The University of Southern Queensland gun tunnel facility was established to complement the higher enthalpy facilities already available at the University of Queensland. The gun tunnel produces test flow durations on the order of tens of milliseconds and hence provides the opportunity to explore unsteady hypersonic flow features not readily accessible in the other facilities at The University of Queensland.

Appropriate instrumentation is required for hypersonic experiments. Static and Pitot pressure measurement, and transient heat flux measurements are routinely obtained. Flow visualization also greatly enhances the understanding of key processes in hypersonic experiments. However, the budget for establishing the USQ gun tunnel facility did not stretch to the acquisition of a commercial multiple-frame system, so an alternative solution was sought. The solution described in this paper is a Cranz-Schardin system. The Cranz-Schardin principle has been used in solid- and fluid mechanics research for over 70 years and it allows dynamic events to be captured at high framing rates through the sequential illumination of the subject from separate light sources (Lu and Liu, 1997).

28th International Congress on High-Speed Imaging and Photonics, edited by Harald Kleine, Martha Patricia Butrón Guillén,
Proc. of SPIE Vol. 7126, 71260G · © 2009 SPIE · CCC code: 0277-786X/09/$18 · doi: 10.1117/12.822032

2. GUN TUNNEL, GAS INJECTION SYSTEM, AND CONE MODEL

Figure 1 illustrates the USQ gun tunnel facility. A primary aluminium diaphragm initially separates the high pressure driver gas from the barrel. The test gas is initially in the barrel and is separated from the test section and aerodynamic model by a secondary, light diaphragm. When the primary diaphragm is ruptured, a piston accelerates into the driver gas and generates a sequence of compression waves which coalesce into a shock wave. The shock reflects off the downstream end of the barrel and decelerates the piston; a sequence of wave reflections occurs as the piston moves down the barrel towards the nozzle throat. Principal dimensions of the gun tunnel facility are presented in Table 1.

(a) Schematic illustration of the facility

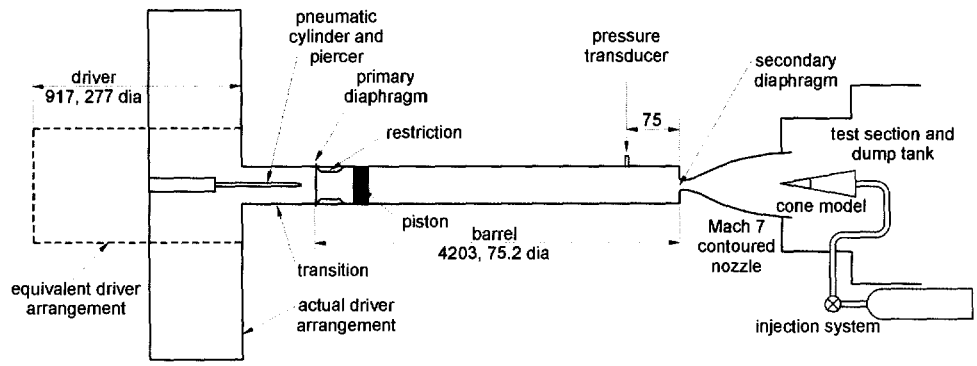

(b) Annotated photograph of facility

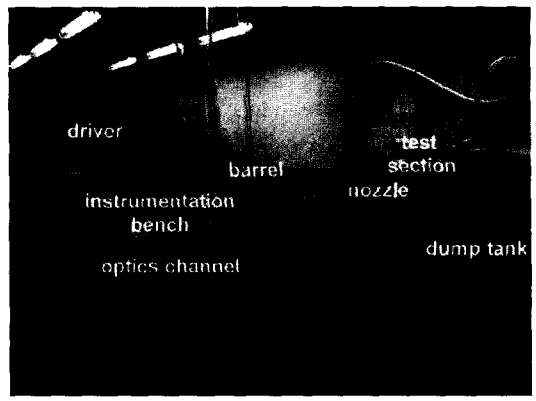

Fig. 1. Gun tunnel facility and arrangement of experiments: (a) schematic illustration of gun tunnel and cone model, dimensions in mm; (b) annotated photograph.

The stagnation pressure produced by the gun tunnel for the present operating condition is shown in Fig. 2a. Flow conditions produced in the facility can be estimated from an isentropic analysis because, although the shock compression raises the entropy of the test gas, the gains are modest and are attenuated by the heat transfer from the compressed test gas to the walls of the barrel. Images were obtained within the region indicated as the "test time" on Fig. 2a.

The model used in the experiments was a 10 degree half angle cone with the option for gas injection through an annulus as illustrated in Fig. 3. The width of the annulus was adjustable, but for the experiments reported here, it was set to 0.43 mm. The model was positioned on the centerline of the Mach 7 nozzle at zero angle of attack. The gas supply system consisted of a fast-acting valve, a gas supply bottle, and associated ¾" plumbing. At the appropriate time, just prior to rupture of the main diaphragm in the gun tunnel, the fast-acting valve was opened and air from the bottle was piped towards the annulus through the base of the cone. Gas injection pressure was monitored using a transducer in the base of the cone. Figure 2b illustrates the pressure recorded from the gas injection pressure transducer.

Table 1. Components of USQ gun tunnel

Component	Characteristics (dimensions, mm)
Driver	277 dia.[1], 917 long, 0.055 m^3
Transition[2]	308 long
Diaphragm	Aluminium, mechanically pierced
Restriction	57.7 dia., 60 long
Barrel	75.2 dia., 4203 long
Piston	61 grams
Nozzle	M7, 87 exit dia., 390 long
Test section	300 × 300, 300 long
Dump tank	500 dia., 3020 long

1. Effective diameter giving actual driver volume due to "T" arrangement of driver and barrel, see Fig. 1.
2. Transition from driver diameter to restriction, see Fig. 1.

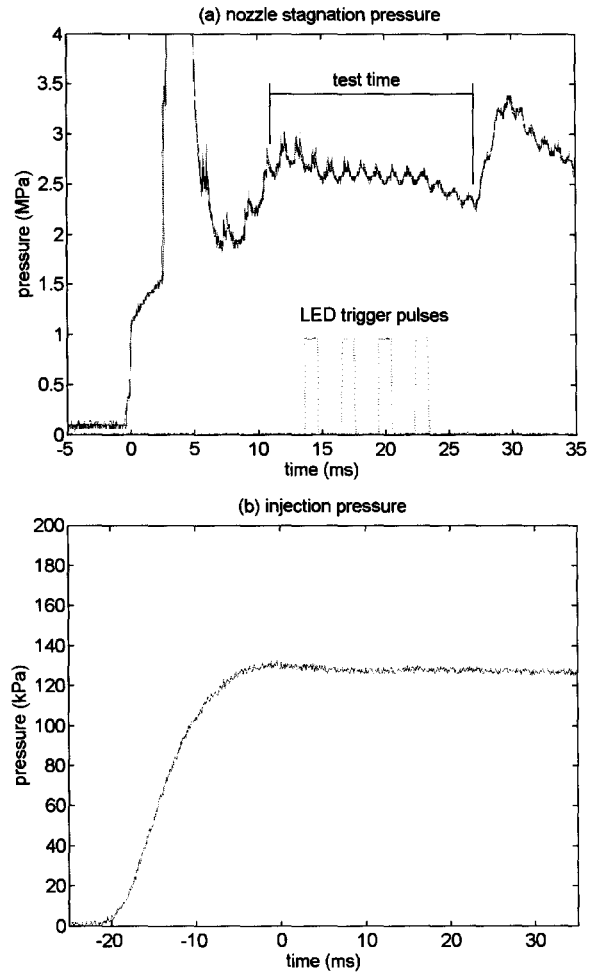

Fig. 2. Pressure measurements: (a) the gun tunnel nozzle stagnation pressure; and (b) the gas injection system. The LEDs were sequenced using the leading edges of the trigger pulses shown in part (a).

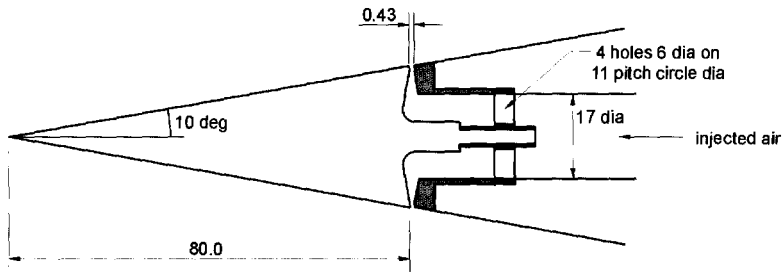

Fig. 3. Illustration of the 10 degree half angle cone model with annular slot for gas injection. Dimensions in mm.

3. OPTICAL SYSTEM

The optical arrangement is illustrated in Fig. 4. Five LED light sources were used and each LED was powered by a separate unit of the type described in Buttsworth and Ahfock (2003). The timing of each LED pulse was controlled by a HC11 microprocessor. The image from the on-axis light source was recorded on a digital still camera. Images from the four off-axis LEDs were recorded using black and white video cameras. Mirrors were used to direct the off-axis light sources to their respective cameras.

(a) Illustration showing optical arrangement of system

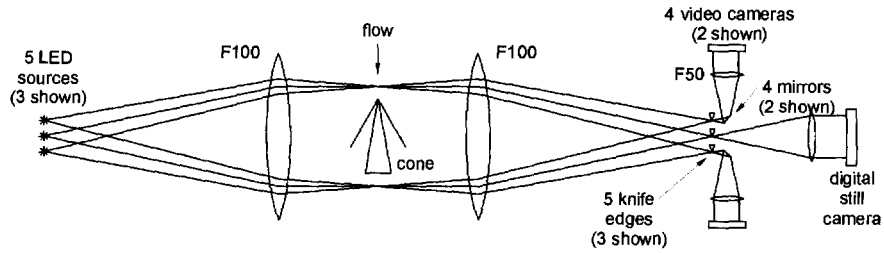

(b) Photograph showing arrangement of cameras

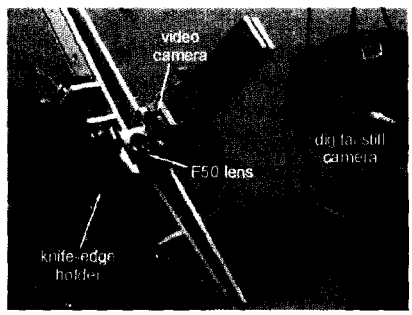

Fig. 4. Optical arrangement: (a) schematic illustration; (b) photograph showing arrangement of video cameras and digital still camera.

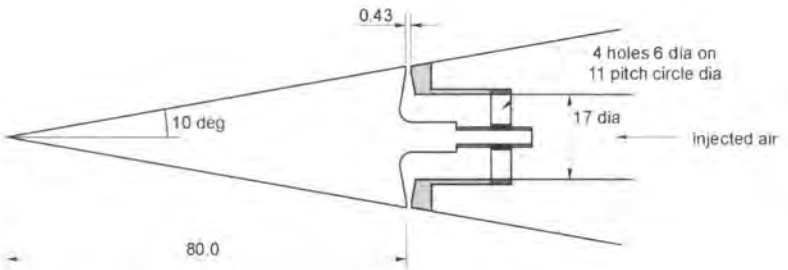

Fig. 3. Illustration of the 10 degree half angle cone model with annular slot for gas injection. Dimensions in mm.

3. OPTICAL SYSTEM

The optical arrangement is illustrated in Fig. 4. Five LED light sources were used and each LED was powered by a separate unit of the type described in Buttsworth and Ahfock (2003). The timing of each LED pulse was controlled by a HC11 microprocessor. The image from the on-axis light source was recorded on a digital still camera. Images from the four off-axis LEDs were recorded using black and white video cameras. Mirrors were used to direct the off-axis light sources to their respective cameras.

(a) Illustration showing optical arrangement of system

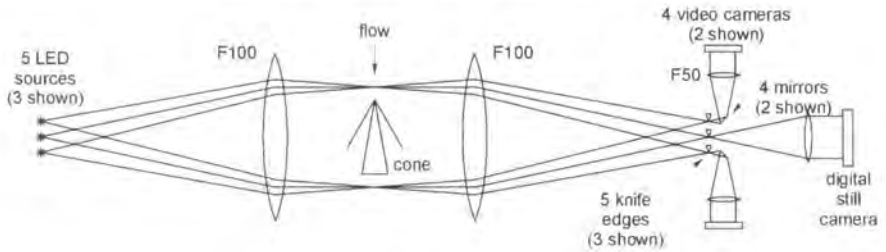

(b) Photograph showing arrangement of cameras

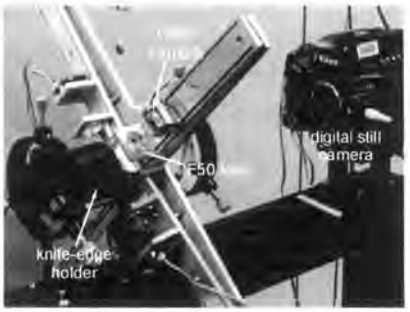

Fig. 4. Optical arrangement: (a) schematic illustration; (b) photograph showing arrangement of video cameras and digital still camera.

4. RESULTS AND IMAGE ANALYSIS

A no-flow photograph of the cone is presented in Fig. 5. In this image, a grid pattern can also be seen. This grid of lines was printed onto a transparent sheet which was placed near the centre line of the test section and was photographed using each camera. Images of the no-flow grid pattern were used in subsequent analysis to digitally correct the off-axis images for distortion. At the left-vertical edge of the visible region on the image of Fig. 5, the Mach 7 nozzle exit can be seen.

Fig. 5. No-flow image showing grid used to correct for image-distortion.

Although the majority of our experiments were performed using LED light sources, some experiments were performed to test the suitability of laser diode light sources. A sample image of the cone flow without gas injection is presented in Fig. 6. For this image, a current pulse width of approximately 1.5 microseconds was supplied to the laser diode. From Fig. 6, the shock angle was measured at 13.9 degrees. The Taylor-Maccoll 10 degree half angle cone flow solution for air (perfect gas) at Mach 7 indicates a 12.9 degree shock angle. Boundary layers on both the Mach 7 nozzle and on the cone are likely contributors to this discrepancy. The hypersonic nozzle used in these experiments was designed to produce a Mach 7 flow at a considerably higher Reynolds number than used in the present experiments, and the Taylor-Maccoll solution is for inviscid cone flow.

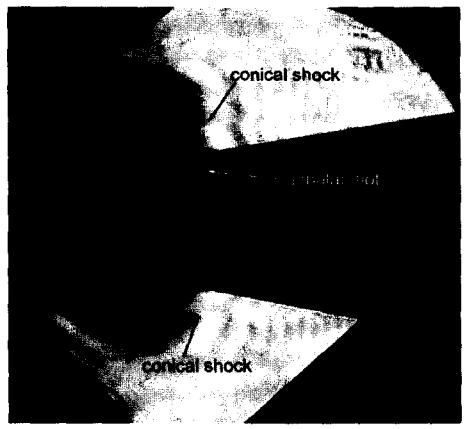

Fig. 6. Vertical knife-edge Schlieren image for a case of no gas injection using laser diode light sources.

4. RESULTS AND IMAGE ANALYSIS

A no-flow photograph of the cone is presented in Fig. 5. In this image, a grid pattern can also be seen. This grid of lines was printed onto a transparent sheet which was placed near the centre line of the test section and was photographed using each camera. Images of the no-flow grid pattern were used in subsequent analysis to digitally correct the off-axis images for distortion. At the left-vertical edge of the visible region on the image of Fig. 5, the Mach 7 nozzle exit can be seen.

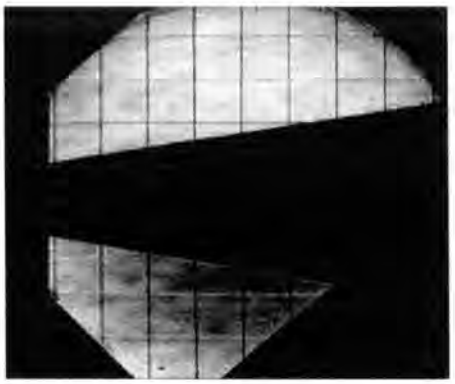

Fig. 5. No-flow image showing grid used to correct for image-distortion.

Although the majority of our experiments were performed using LED light sources, some experiments were performed to test the suitability of laser diode light sources. A sample image of the cone flow without gas injection is presented in Fig. 6. For this image, a current pulse width of approximately 1.5 microseconds was supplied to the laser diode. From Fig. 6, the shock angle was measured at 13.9 degrees. The Taylor-Maccoll 10 degree half angle cone flow solution for air (perfect gas) at Mach 7 indicates a 12.9 degree shock angle. Boundary layers on both the Mach 7 nozzle and on the cone are likely contributors to this discrepancy. The hypersonic nozzle used in these experiments was designed to produce a Mach 7 flow at a considerably higher Reynolds number than used in the present experiments, and the Taylor-Maccoll solution is for inviscid cone flow.

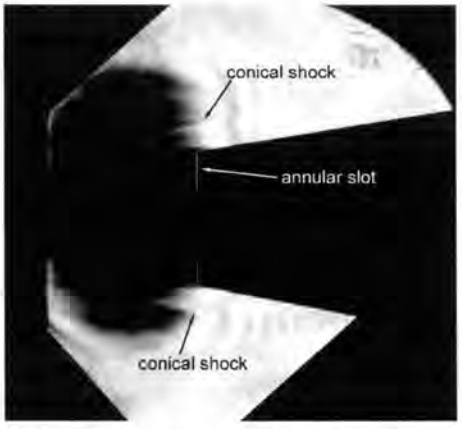

Fig. 6. Vertical knife-edge Schlieren image for a case of no gas injection using laser diode light sources.

Some images were also obtained using the LED sources but with the Schlieren knife edges removed to give a shadowgraph configuration. Fig. 7 illustrates one such image which was obtained with a current pulse to the LED of around 1 μs and gas injection through the annulus. The shock and other flow structures observed in this image (Fig. 7) contrast with the straight conical shock observed with no gas injection (Fig. 6).

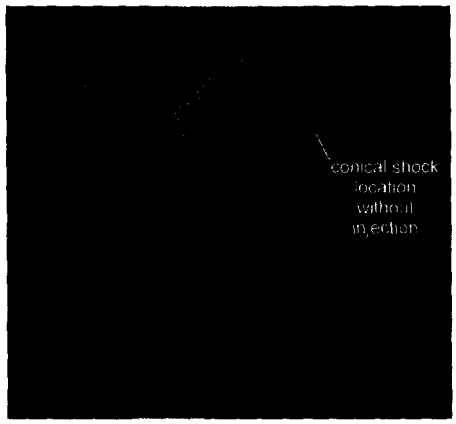

Fig. 7. Shadowgraph with LED illumination and microsecond exposure time.

A sequence of 4 horizontal knife-edge Schlieren images each separated in time by about 3 ms for a single gun tunnel run is presented in Fig. 8. For these images, the LED current pulse width was 10 μs. Some unsteadiness in the shock waves can be observed, although the variations in flow structure are not as obvious as in the case of the shadowgraph of Fig. 7. The Mach 7 flow speed was approximately 1 km/s for these experiments so an effective exposure of 10 μs equates to a free stream travel distance of 10 mm. Hence unsteady structures smaller than 10 mm are likely to be smeared.

The level of unsteadiness observed in the Schlieren images for two different injection cases is summarized in Table 2. In this table, q refers to the ratio of injection to free stream momentum flux,

$$q = \frac{\rho_{inj} U_{inj}^2}{\rho_\infty U_\infty^2} \tag{1}$$

where ρ is flow density, U is flow velocity and subscripts *inj* and ∞ refer to the conditions at injection and in the free stream flow. The ratio of injection to free-stream momentum flux and is often used as a correlating parameter for transverse injection studies (Schetz, 1980).

Some images were also obtained using the LED sources but with the Schlieren knife edges removed to give a shadowgraph configuration. Fig. 7 illustrates one such image which was obtained with a current pulse to the LED of around 1 μs and gas injection through the annulus. The shock and other flow structures observed in this image (Fig. 7) contrast with the straight conical shock observed with no gas injection (Fig. 6).

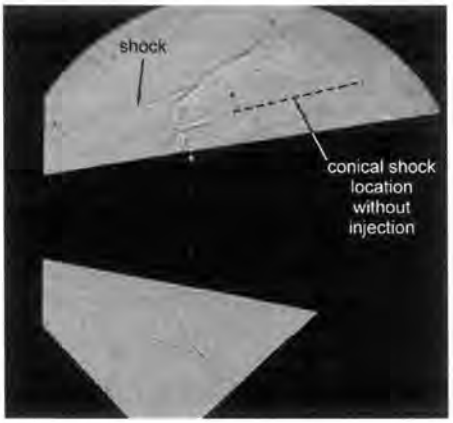

Fig. 7. Shadowgraph with LED illumination and microsecond exposure time.

A sequence of 4 horizontal knife-edge Schlieren images each separated in time by about 3 ms for a single gun tunnel run is presented in Fig. 8. For these images, the LED current pulse width was 10 μs. Some unsteadiness in the shock waves can be observed, although the variations in flow structure are not as obvious as in the case of the shadowgraph of Fig. 7. The Mach 7 flow speed was approximately 1 km/s for these experiments so an effective exposure of 10 μs equates to a free stream travel distance of 10 mm. Hence unsteady structures smaller than 10 mm are likely to be smeared.

The level of unsteadiness observed in the Schlieren images for two different injection cases is summarized in Table 2. In this table, q refers to the ratio of injection to free stream momentum flux,

$$q = \frac{\rho_{inj} U_{inj}^2}{\rho_\infty U_\infty^2} \qquad (1)$$

where ρ is flow density, U is flow velocity and subscripts *inj* and ∞ refer to the conditions at injection and in the free stream flow. The ratio of injection to free-stream momentum flux and is often used as a correlating parameter for transverse injection studies (Schetz, 1980).

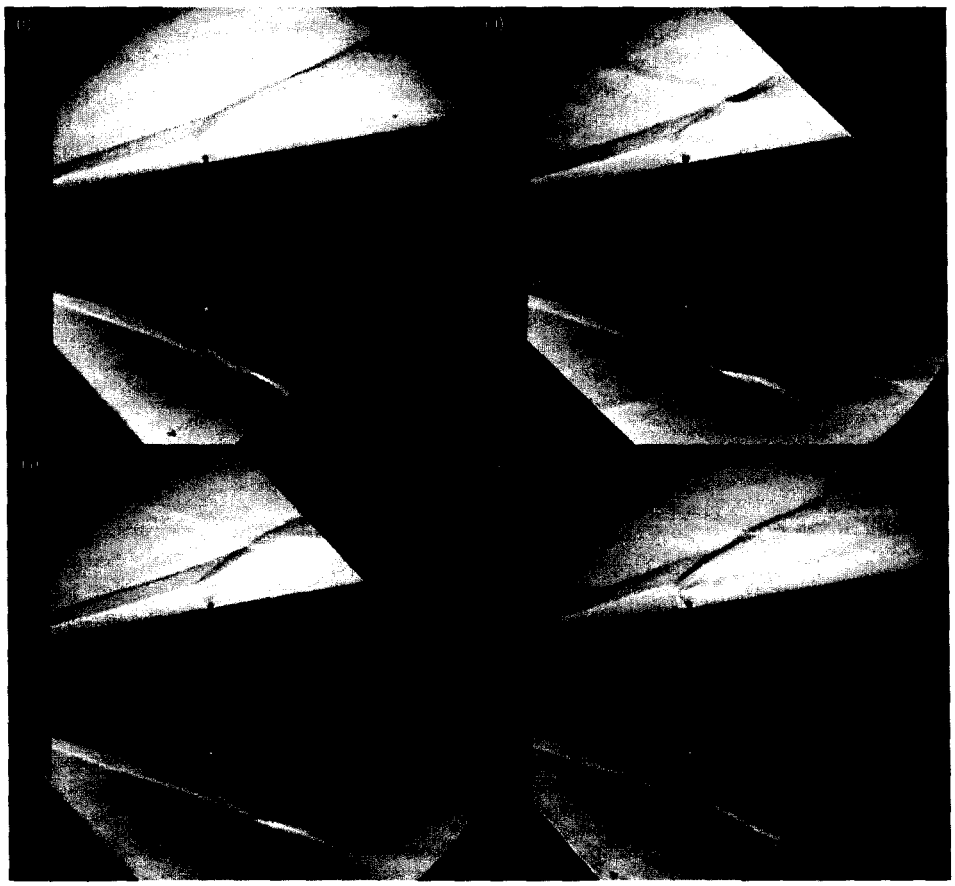

Fig. 8. Sequence of vertical knife-edge Schlieren images for a case of gas injection with $q = 2.1$.

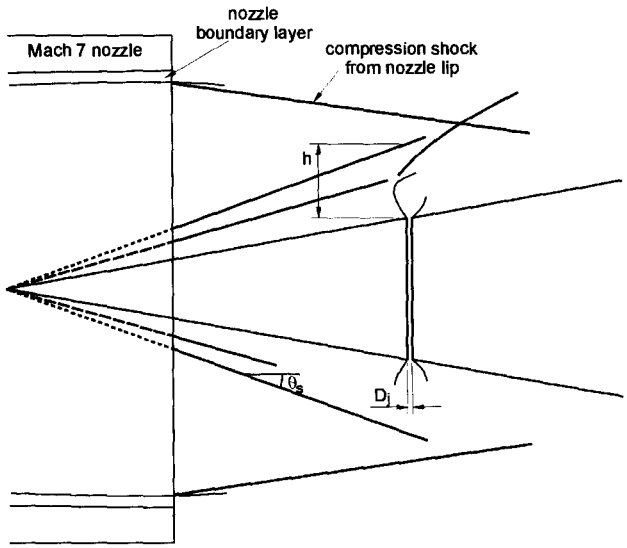

Fig. 9. Definition of shock height h, annular gap D_j, and shock angle θ_s.

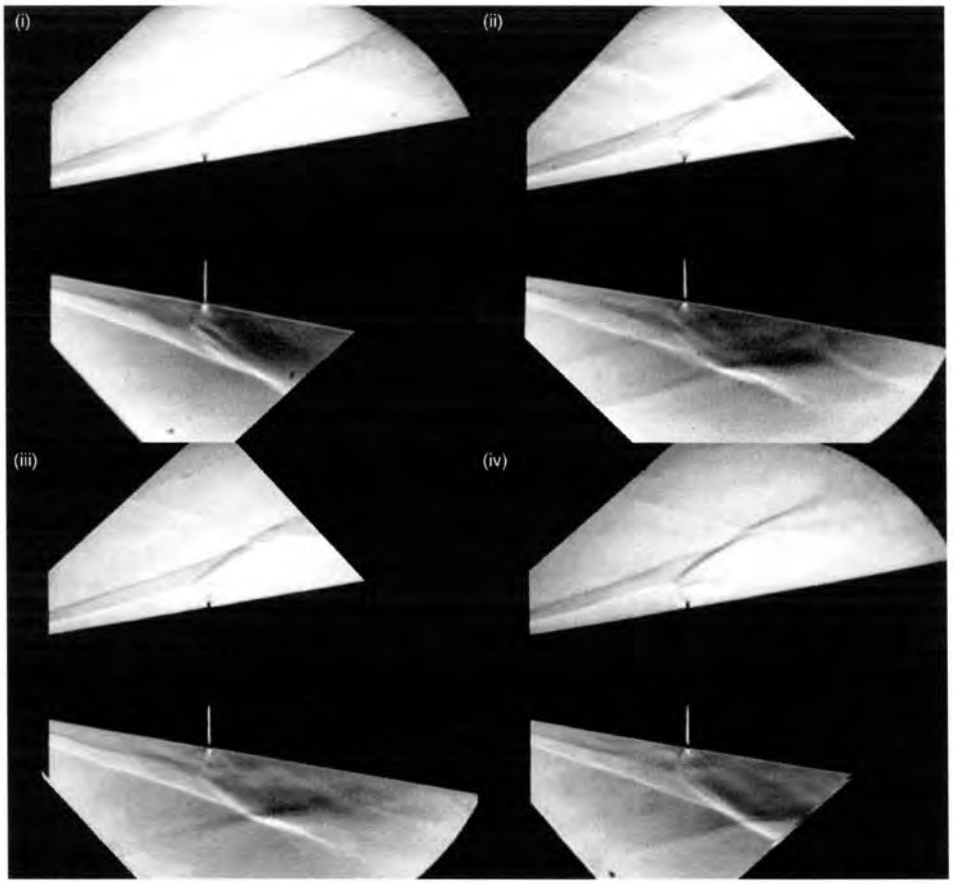

Fig. 8. Sequence of vertical knife-edge Schlieren images for a case of gas injection with $q = 2.1$.

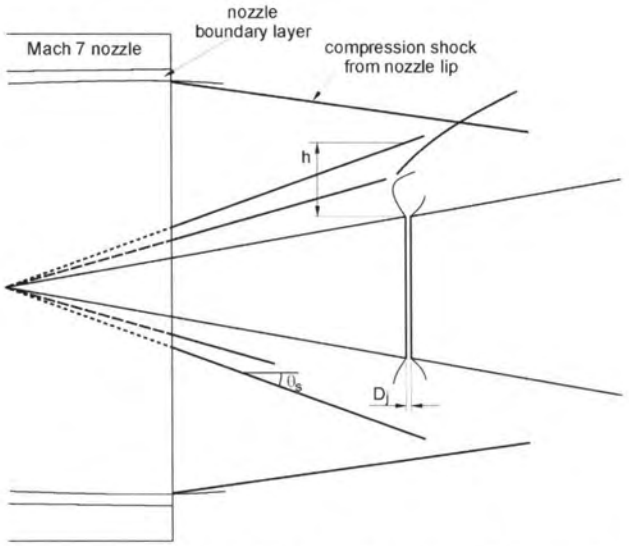

Fig. 9. Definition of shock height h, annular gap D_j, and shock angle θ_s.

In Table 2, the quantity h was determined by plotting a vertical line at the approximate centre of the annular gap and picking the points that intersected the face of the cone and the edge of the main bounding shock around the cone model as illustrated in Fig. 9. The quantity D_j is the axial gap in the annulus (0.43 mm for the present experiments). Note that the shock angles in the injection cases are much higher than the no-injection case. It appears likely that the region of separated flow ahead of the annular injection is disturbing the conical shock wave upstream of the limits of visualization.

Table 2. Shock measurements from the Schlieren images.

Δt (ms)	q = 3.5 (Run 35)		q = 2.1 (Run 36)	
	θ_s (deg)	h/D_j	θ_s (deg)	h/D_j
0	19.2	27.2	19.0	23.6
3	18.5	28.5	19.1	25.1
6	19.5	27.3	18.4	23.6
9	18.2	28.5	18.2	24.7

5. CONCLUSION

A low cost, multiple image flow visualization system for the University of Southern Queensland gun tunnel has been developed and demonstrated for the case of gas injection from an annulus on a 10 degree half angle cone. The conical shock appeared very steady when there was no injection from the annulus. Therefore, the strong unsteadiness observed in the shock wave structures when gas injection was employed is related to the injected gas and not the variations in the free stream flow produced by the gun tunnel. The conical shock is influenced by the separated flow region ahead of the annulus. This region of influence extends far upstream, beyond the limits of visualization. The cone tip region should be visualized in future work so that the extent of the separated flow region and its influence on the conical shock can be determined.

REFERENCES

[1] Stalker, R. J., "Modern developments in hypersonic wind tunnels", Aeronautical Journal, Vol. 110 (1103), 21–39 (2006)

[2] Lu, F. K., Liu, X., "Optical design of Cranz-Schardin cameras", *Opt. Eng.* 36(7) 1935–1941 (July 1997)

[3] Schetz, J. A., Injection and Mixing in Turbulent Flows, Vol. 68, Progress in Astronautics and Aeronautics, AIAA, Chapter 8, pp. 154-160 (1980).

[4] Buttsworth, D. R., Ahfock, A. L., "A Pulsed LED system for Schlieren flow visualization," Faculty of Engineering and Surveying Technical Reports, TR-2003-01 (2003)